ELSEVIER

JMB

Volume 402, Issue 3

Contents

Review

The miR-15/107 Group of MicroRNA Genes: Evolutionary Biology, Cellular Functions, and Roles in Human Diseases	**J. R. Finnerty, W.-X. Wang, S. S. Hébert, B. R. Wilfred, G. Mao and P. T. Nelson**	491–509

Articles

Chloroplast Import Signals: The Length Requirement for Translocation *In Vitro* and *In Vivo*	**T. Bionda, B. Tillmann, S. Simm, K. Beilstein, M. Ruprecht and E. Schleiff**	510–523
Structural Insight into the Mechanism of c-di-GMP Hydrolysis by EAL Domain Phosphodiesterases	**A. Tchigvintsev, X. Xu, A. Singer, C. Chang, G. Brown, M. Proudfoot, H. Cui, R. Flick, W. F. Anderson, A. Joachimiak, M. Y. Galperin, A. Savchenko and A. F. Yakunin**	524–538
Urate Is a Ligand for the Transcriptional Regulator PecS	**I. C. Perera and A. Grove**	539–551
Crystal Structure of the Cyanobacterial Signal Transduction Protein P_{II} in Complex with PipX	**M.-X. Zhao, Y.-L. Jiang, B.-Y. Xu, Y. Chen, C.-C. Zhang and C.-Z. Zhou**	552–559
Structure of the AML1-ETO NHR3–PKA(RIIα) Complex and Its Contribution to AML1-ETO Activity	**T. Corpora, L. Roudaia, Z. M. Oo, W. Chen, E. Manuylova, X. Cai, M. J. Chen, T. Cierpicki, N. A. Speck and J. H. Bushweller**	560–577
H-Bonding and Positive Charge at the N(5)/O(4) Locus Are Critical for Covalent Flavin Attachment in *Trametes* Pyranose 2-Oxidase	**T.-C. Tan, W. Pitsawong, T. Wongnate, O. Spadiut, D. Haltrich, P. Chaiyen and C. Divne**	578–594
Effects of Turn Stability and Side-Chain Hydrophobicity on the Folding of ß-Structures	**Q. Shao, H. Wei and Y. Q. Gao**	595–609
Measuring "Unmeasurable" Folding Kinetics of Proteins by Single-Molecule Force Spectroscopy	**A. Jollymore and H. Li**	610–617

Abstracted/indexed in: BIOSIS, Biochemistry and Biophysics Citation Index, Biological Abstracts, Biological and Agricultural Index, Biostatistica, Biotechnology Citation Index, Chemical Abstracts, Current Contents (Life Sciences, Clinical Medicine), EMBASE, EMBiology, Excerpta Medica, Food Science and Technology Abstracts, Genetics Abstracts, Immunology Abstracts, MEDLINE®, Reference Update, Research Alert, SCISEARCH, Science Citation Index, etc. Also covered in the abstract and citation database SCOPUS®. Full text available on ScienceDirect®

doi:10.1016/j.jmb.2010.08.006 J. Mol. Biol. (2010) 402, 552–559

Contents lists available at www.sciencedirect.com

Journal of Molecular Biology

journal homepage: http://ees.elsevier.com.jmb

Crystal Structure of the Cyanobacterial Signal Transduction Protein P_{II} in Complex with PipX

Meng-Xi Zhao[1]†, Yong-Liang Jiang[1]†, Bo-Ying Xu[1], Yuxing Chen[1], Cheng-Cai Zhang[2] and Cong-Zhao Zhou[1]*

[1]*Hefei National Laboratory for Physical Sciences at Microscale and School of Life Sciences, University of Science and Technology of China, Hefei, Anhui 230027, People's Republic of China*
[2]*Aix-Marseille Université and Laboratoire de Chimie Bactérienne, Unités Propres de Recherche 9043, Centre National de la Recherche Scientifique, 31 Chemin Joseph Aiguier, 13402 Marseille Cedex 20, France*

Received 25 June 2010; received in revised form 1 August 2010; accepted 4 August 2010
Available online 12 August 2010

Edited by K. Morikawa

Keywords:
cyanobacteria;
signal transducers;
PII;
PipX;
2-oxoglutarate

P_{II} proteins are highly conserved signal transducers in bacteria, archaea, and plants. They have a large flexible loop (T-loop) that adopts different conformations after covalent modification or binding to different effectors to regulate the functions of diverse protein partners. The P_{II} partner PipX (P_{II} *i*nteraction *p*rotein *X*), first identified from *Synechococcus* sp. PCC 7942, exists uniquely in cyanobacteria. PipX also interacts with the cyanobacterial global nitrogen regulator NtcA. The mutually exclusive binding of P_{II} and NtcA by PipX in a 2-oxoglutarate (2-OG)-dependent manner enables P_{II} to indirectly regulate the transcriptional activity of NtcA. However, the structural basis for these exclusive interactions remains unknown. We solved the crystal structure of the P_{II}–PipX complex from the filamentous cyanobacterium *Anabaena* sp. PCC 7120 at 1.90 Å resolution. A homotrimeric P_{II} captures three subunits of PipX through the T-loops. Similar to P_{II} from *Synechococcus*, the core structure consists of an antiparallel β-sheet with four β-strands and two α-helices at the lateral surface. PipX adopts a novel structure composed of five twisted antiparallel β-strands and two α-helices, which is reminiscent of the P_{II} structure. The T-loop of each P_{II} subunit extends from the core structure as an antenna that is stabilized at the cleft between two PipX monomers via hydrogen bonds. In addition, the interfaces between the β-sheets of PipX and P_{II} core structures partially contribute to complex formation. Comparative structural analysis indicated that PipX and 2-OG share a common binding site that overlaps with the 14 signature residues of cyanobacterial P_{II} proteins. Our structure of PipX and the recently solved NtcA structure enabled us to propose a putative model for the NtcA–PipX complex. Taken together, these findings provide structural insights into how P_{II} regulates the transcriptional activity of NtcA via PipX upon accumulation of the metabolite 2-OG.

Introduction

P_{II} signaling proteins are highly conserved in bacteria, archaea, and plants. Genes coding for P_{II} proteins are divided into three subfamilies: *glnB*, *glnK*, and *nifI*.[1] GlnB and GlnK function as homotrimers to modulate nitrogen assimilation. Heterotrimeric NifI is distinct from the members of the

*Corresponding author. E-mail address: zcz@ustc.edu.cn.
† M.-X.Z. and Y.-L.J. contributed equally to this work.
Abbreviations used: 2-OG, 2-oxoglutarate; NAGK, *N*-acetyl glutamate kinase; PDB, Protein Data Bank.

other two subfamilies and is found only in nitrogen-fixing archaea and some anaerobic bacteria.[2] P_{II} proteins sense carbon-related, nitrogen-related, and energy-related signals, and interact with diverse target proteins, most of which are involved in the regulation of nitrogen metabolism. A series of structures of P_{II} proteins from bacteria,[3–7] archaea,[8] and plants[9] have been solved. All exist as trimers, with each subunit sharing a highly similar core structure of an antiparallel β-sheet and two α-helices at the lateral surface. The three subunits form a short cylinder, with the functional large flexible loop (T-loop) of each subunit protruding towards the solvent as an antenna to interact with the partner proteins. Most P_{II} proteins sense signals in two modes: through effector-triggered conformational changes and through covalent modifications.[10] Both modes are primarily dependent on the variable T-loop. The binding pattern of the effectors ATP/ADP and 2-oxoglutarate (2-OG) is universal and conserved among P_{II} proteins.[1,11–13] These effectors enable the T-loop to adopt different conformations for interacting with diverse P_{II} partners.[10] ATP is stabilized at the intersubunit cleft of P_{II},[14] and its binding is synergistic with the association of 2-OG.[15] In contrast, the covalent modification patterns are less conserved. Residue Ser49 of P_{II} from the unicellular cyanobacterium *Synechococcus elongatus* PCC 7942 (referred to as *Synechococcus*) or *Synechocystis* PCC 6803 (referred to as *Synechocystis*) is phosphorylated under poor nitrogen conditions,[11] while Tyr51 is nitrificated in the heterocystous cyanobacterium *Anabaena* sp. PCC 7120 (referred to as *Anabaena*).[16] In *Escherichia coli*, P_{II} is regulated by uridylylation at the conserved Tyr51 residue of the T-loop.[17]

To date, only GlnB-type P_{II} has been found in all sequenced cyanobacteria.[18] Because of the absence of 2-OG dehydrogenase in cyanobacteria,[19] the 2-OG produced by the Krebs cycle serves mainly as a carbon skeleton for nitrogen assimilation through the glutamine synthetase–glutamate synthase pathway. The direct link of 2-OG level to nitrogen assimilation makes the metabolite 2-OG an important signal of the carbon/nitrogen balance in cyanobacteria, and this signal is sensed by P_{II} protein.

Three P_{II} partner proteins have been reported in cyanobacteria: *N*-acetyl glutamate kinase (NAGK)[20] and PipX (P_{II} *i*nteraction *p*rotein *X*) in *Synechococcus*,[20,21] and the membrane protein PamA of unknown function in *Synechocystis*.[22] Of these, only the molecular mechanism of NAGK regulation by P_{II} has been clearly illustrated from the structural point of view.[23] After being first identified in *Synechococcus*,[20,21] PipX has been found exclusively in all cyanobacteria. It specifically interacts only with cyanobacterial P_{II}, and not with *E. coli* GlnB or GlnK, or with *Arabidopsis thaliana* P_{II}.[21] PipX also interacts with the global nitrogen regulator NtcA,[21] which belongs to the Crp/Fnr transcription factor family and regulates a group of cyanobacterial nitrogen assimilation genes. PipX switches between binding P_{II} and binding NtcA, depending on the cellular 2-OG concentration.[21,24] At lower 2-OG concentrations, PipX is bound to P_{II}. Upon 2-OG accumulation, PipX binds to NtcA.[21] 2-OG impairs the interaction between P_{II} and PipX in the presence of ATP, but facilitates the formation of the NtcA–PipX complex. The three proteins P_{II}, PipX, and NtcA are highly conserved in all sequenced cyanobacterial genomes, and NtcA and PipX are exclusively encoded by cyanobacteria, indicating that the 2-OG-dependent swapping of PipX might be a universal mechanism of cyanobacteria.

Here, we present the structure of the P_{II}–PipX complex from *Anabaena*. After the structures of the P_{II}–NAGK complex[23,25] and the AmtB–GlnK[26] complex, our structure represents the third complex of P_{II} with its partner. P_{II} assembles into a trimer as reported and interacts with PipX through the T-loops. The homotrimer of P_{II} resembles an upside-down tripod that holds three PipX molecules, which have only slight interactions with each other. Through comparative structural analysis, we deduced how 2-OG and ATP/ADP affect the interaction between P_{II} and PipX. Further structural simulation provides insight into the swapping of PipX from P_{II} to NtcA.

Results

Overall structure of the P_{II}–PipX complex

The structure of the P_{II}–PipX complex was solved and refined to 1.90 Å resolution. It belongs to space group *P*321, with unit cell dimensions of $a = 70.65$ Å, $b = 70.65$ Å, $c = 88.54$ Å, $\alpha = 90.00°$, $\beta = 90.00°$, and $\gamma = 120.00°$. The asymmetric unit contains one molecule each of P_{II} and PipX, which form a 3-fold symmetric complex with a stoichiometry of 3 P_{II}:3 PipX (Fig. 1a and b). The overall structure of the complex resembles a triangular prism that is 43 Å in height and 64 Å (for the PipX layer) or 40 Å (for the P_{II} layer) in width. Each P_{II} subunit inserts its well-ordered T-loop (Phe36-Leu56) into the lateral cleft of two adjacent PipX molecules, stabilizing the complex via extensive contacts. Three subunits of PipX form a positively charged hole at the center of the P_{II} trimer (Fig. 1c).

Structural comparison of P_{II}

Anabaena P_{II} adopts a ferredoxin-like fold (Fig. 2a), as defined by the Structural Classification of Proteins‡. The overall structure is very similar to the

‡ http://scop.berkeley.edu/data/scop.b.e.bcj.html

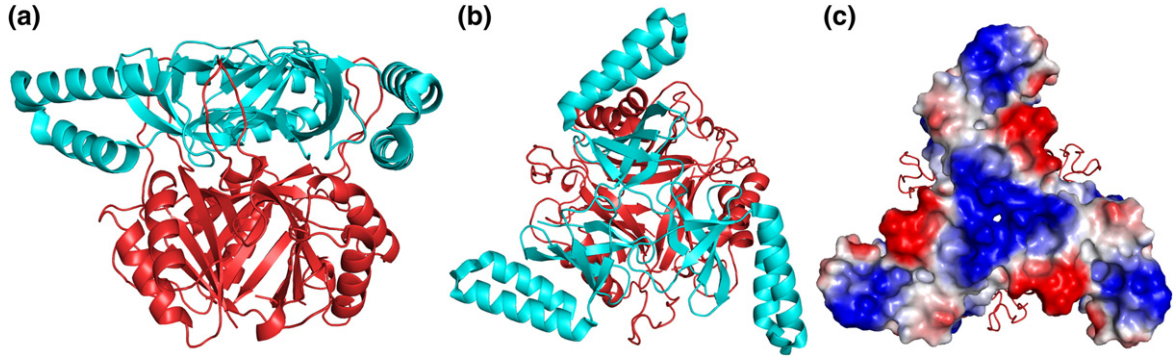

Fig. 1. Overall structure of the P_{II}–PipX complex. (a) Side view of the complex. P_{II} is shown in red, and PipX is shown in cyan. Top view of the complex, with PipX shown as (b) cartoon and (c) electrostatic potential.

previously reported cyanobacterial P_{II}[5] and *E. coli* GlnK.[14] Three P_{II} molecules form a tight cylindrical trimer, with each subunit containing the central four-stranded β-sheet surrounded at the outer surface by two α-helices. The central β-sheets of the trimer form an intersubunit interface with a total area of 3300 $Å^2$. However, the T-loop exhibits a conformation distinct from those previously reported for either free P_{II} or complexed P_{II}.[5,8,14,23,26,27] The T-loops in most free P_{II} structures reported to date are disordered because of their high level of flexibility, but adopt different conformations in which they point to different directions upon binding to their effectors or partners (Fig. 2b). In our structure, the T-loop exhibits an extended and ordered conformation, protruding approximately 25 Å from the core structure (Fig. 2a).

Despite the fact no nucleotide was introduced during protein purification or crystallization, an ADP molecule was observed at the lateral cleft of two adjacent P_{II} molecules. The ADP should be incorporated into P_{II} during overexpression in *E. coli*. Previous structures have shown that both ADP and ATP can bind to the corresponding site in *E. coli* GlnK[8,14] and GlnB.[5] Recent crystal structures of the AmtB–GlnK complex[26,27] also revealed an ADP molecule buried at the nucleotide binding site. Superposition of our P_{II} structure onto GlnK from the AmtB–GlnK complex structure showed that the ADP molecules superimposed, while the T-loops adopted different orientations, although all extended out from the core (Fig. 2c). The ADP molecule is almost completely buried in the lateral cleft, and the hydrogen-bonding pattern with the base and sugar phosphate moieties of the ADP is very similar to that of the AmtB–GlnK complex.

Novel structure of PipX

PipX is a small protein of about 90 residues (unique to cyanobacteria) that functions as a transcriptional coactivator of NtcA.[21] To our surprise, the overall structure of PipX is reminiscent of P_{II}, despite their different topologies. PipX also consists of a twisted

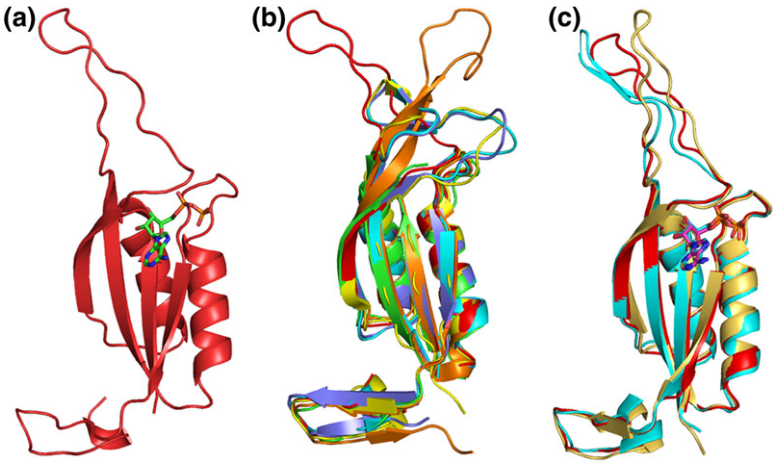

Fig. 2. (a) Structure of P_{II}. The ADP bound to P_{II} is shown as a stick model and colored by element. (b) Different conformations of T-loops. *Anabaena* P_{II} in complex with PipX is shown in red, *M. jannaschii* GlnK bound to ATP is shown in cyan (PDB code 2J9E), *M. jannaschii* GlnK bound to Mg-ATP and 2-OG is shown in yellow (PDB code 2J9E), *Synechococcus* free P_{II} is shown in orange (PDB code 1QY7), *Synechococcus* P_{II} complexed with NAGK is shown in blue (PDB code 2V5H), and *E. coli* GlnK bound to ATP is shown in green (PDB code 2GNK). (c) Superposition of PipX-complexed P_{II} (red) to ADP-bound P_{II} proteins. *E. coli* GlnK in complex with AmtB is shown in cyan (PDB code 2NS1), and *M. jannaschii* ADP-bound GlnK is shown in yellow (PDB code 2J9D).

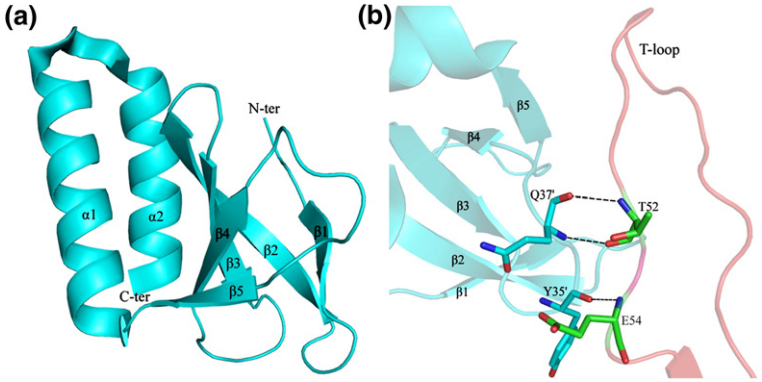

Fig. 3. (a) Structure of PipX. Secondary structure elements are labeled sequentially. (b) Interactions between the T-loop of P_{II} and PipX. The residues involved in hydrogen bonds are shown as stick models and colored according to atom type. Black dotted lines denote hydrogen bonds, with length expressed in angstroms. The backbone of the protein is presented as a semitransparent cartoon.

antiparallel β-sheet patched on one side by two α-helices (Fig. 3a). Part of the β-sheet (strands β3 and β4, and the second moiety of β2) and the pair of α-helices form an intramolecular interface, while the β-hairpin composed of β1 and the first moiety of β2 form an interface with the central β-sheet of P_{II}. The three pairs of α-helices are arranged into a triangular conformation at the outer surface of the complex (Fig. 1b). The PipX monomer was compared to structures in the Protein Data Bank (PDB§) using the DALI server‖.[28] The output of 211 hits with a *Z*-score higher than 3.0 covered 64 unique proteins of diverse sequences and functions. Of these, the human serine/threonine–protein kinase 16 (PDB code 2BUJ) had the highest *Z*-score (5.0), and the *Dictyostelium discoideum* myosin II heavy chain (PDB code 1YV3) had the most similar sequence, with a 16% identity among the 92 residues of PipX. These results indicate that PipX has a novel structure.

Interfaces between P_{II} and PipX

The trimeric P_{II} buries a total interface area of 2900 $Å^2$ with three subunits of PipX. The interactions are mainly contributed by two patches of each P_{II}. The first patch, from the concave surface of the central β-sheet of P_{II}, interacts with β1 and the first moiety of β2 of PipX. The inter-β-sheet interface buries an area of approximately 540 $Å^2$ per subunit and is mainly composed of hydrogen bonds and salt bridges. The hydrophilic parts of this interface also bury a cluster of well-ordered water molecules. In addition, hydrophobic interactions (Phe11, Leu13, and Leu59 of P_{II}; Leu17, Tyr19, and Leu34 of PipX) partially contribute to further stabilization of this interface. The other patch is provided by the extended T-loop, which acts as an antenna that docks at the lateral cleft between two adjacent PipX subunits. This buries an interface area of about 420 $Å^2$.

§ http://www.rcsb.org/pdb/
‖ http://ekhidna.biocenter.helsinki.fi/dali_server/

The three hydrogen bonds with the loop between β3 and β4 of PipX help maintain the T-loop in an extended conformation. Specifically, Thr52 N^{α} forms a hydrogen bond with the carbonyl oxygen of PipX Gln37, and the Thr52 carbonyl oxygen forms a hydrogen bond with N^{α} of PipX Gln37, while N^{α} of Glu54 makes a hydrogen bond with the carbonyl oxygen of Tyr35 in PipX (Fig. 3b).

Discussion

The interface between P_{II} and PipX is highly conserved

Most cyanobacterial P_{II} proteins share a sequence identity of 50%, and comparison with P_{II} from other bacteria reveals a signature of 14 residues that are exclusively conserved in cyanobacteria.[29] Of these 14 residues, the hydrogen-bonded residues Thr52/Val53 and the hydrophobic Leu59 are critical for stabilizing the P_{II}–PipX complex. The contribution of these signature residues to the P_{II}–PipX interface might explain why PipX specifically binds only to cyanobacterial P_{II} proteins.[21] Multiple alignments of PipX proteins from representative cyanobacteria showed a high conservation of both the hydrogen-bonded residues Tyr35 and Arg38 and the hydrophobic residues Leu17, Tyr19, and Leu34 at the interface with P_{II} (Fig. 4). This suggests that the interaction pattern in our structure of the complex might be applied to all cyanobacterial P_{II}–PipX pairs.

ADP promotes P_{II} capture of PipX by facilitating the extended T-loop conformation

Binding of various effectors such as ADP/ATP and 2-OG affects the conformation of the T-loop and modulates P_{II}–receptor interactions.[8] Structural comparison of our PipX-complexed P_{II} to previous complexed or free P_{II} proteins indicated that they all showed similar overall structures, but different T-loop conformations (Fig. 2b). Several structures of ADP-bound P_{II} have been reported. In *Thermus*

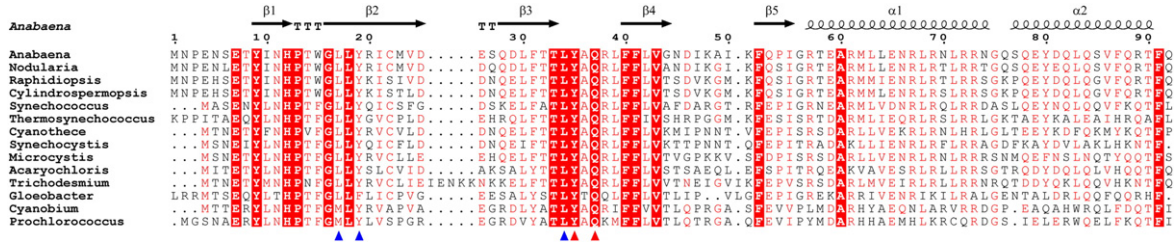

Fig. 4. Sequence alignment of cyanobacterial PipX proteins. P_{II}–PipX interaction residues are labeled. Red triangles show hydrogen-bonding sites, while blue ones show hydrophobic contacts. The sequences of PipX are from the following: *Anabaena*; *Nodularia spumigena* CCY9414; *Raphidiopsis brookii* D9; *Cylindrospermopsis raciborskii* CS-505; *Synechococcus*; *Thermosynechococcus elongatus* BP-1; *Cyanothece* sp. ATCC51142; *Synechocystis*; *Microcystis aeruginosa* NIES-843; *Acaryochloris marina* MBIC11017; *Trichodesmium erythraeum* IMS101; *Gloeobacter violaceus* PCC 7421; *Cyanobium* sp. PCC 7001; *Prochlorococcus marinus* str. MIT 9211.

thermophilus GlnK, ADP was added during crystallization,[6] while in *Thermotoga maritima* P_{II}[30] and *E. coli* AmtB–GlnK complex,[26] ADP was found in the crystal structure without the introduction of nucleotides during purification and crystallization. Another structure of the *E. coli* AmtB–GlnK complex[27] contained ADP in the ATP-binding pocket, although crystallization was carried out in buffer containing ATP. Superposition of our P_{II} structure against *E. coli* GlnK in complex with AmtB, and superposition of our P_{II} structure against *Methanococcus jannaschii* GlnK in complex with ADP revealed that T-loops in all three structures exhibited an ordered extended conformation and a similar orientation (Fig. 2c). All ADP molecules in the binding cleft could be superimposed. Two hydrogen bonds are formed between the N^{α} groups of residues Arg38 and Gln39 at the beginning of the T-loop, and oxygen atoms of the α-phosphate group. These interactions fix a 90° kink at Arg38 and Gln39 that appears to be important for positioning the T-loop in an extended conformation.

Binding of PipX and 2-OG to P_{II} is mutually exclusive

Previous studies showed that P_{II} protein binds 2-OG and ATP synergistically.[31] Binding of ATP fixes the T-loop in its compact conformation, especially in the presence of magnesium ion.[8] The 2-OG binding site was generated with a compact T-loop conformation, but was absent from an extended one. The compact conformation was stabilized by 2-OG.

Crystal structures of *M. jannaschii* GlnK with bound effectors showed for the first time a 2-OG molecule binding to one subunit of the GlnK trimer at the distal site of the compact T-loop that forms upon the binding of Mg-ATP.[8] In our structure, the 2-OG binding site (Thr52, Val53, and Glu54) at the T-loop was occupied by PipX (Fig. 5). Thus, 2-OG is proposed to competitively bind the same site on P_{II}, resulting in the disruption of the P_{II}–PipX interface. This is in agreement with results showing that the accumulation of 2-OG releases PipX from P_{II}.[21]

A model of PipX in complex with 2-OG-bound NtcA

An increase in 2-OG will cause P_{II} to release PipX, which can then bind to NtcA and act as a coactivator of transcription.[21,24] Based on the PipX structure presented here and our previous structure of NtcA in complex with 2-OG,[32] a three-dimensional model of NtcA–PipX complex was simulated using the program HADDOCK.[33] Docking was started with the 2-OG-bound NtcA dimer and the PipX monomer, and was driven by interaction restraints with the active residues, as defined by the program WHISCY.[34] Among the 12 output clusters, the cluster of lowest energy with 13 members satisfied the best interaction restraints and had the largest buried interface area of approximately 1200 $Å^2$ for each PipX monomer. The overall backbone root-mean-square deviation (RMSD) of 1.5 ± 1.4 Å for the 13 members indicated that the model of NtcA–PipX

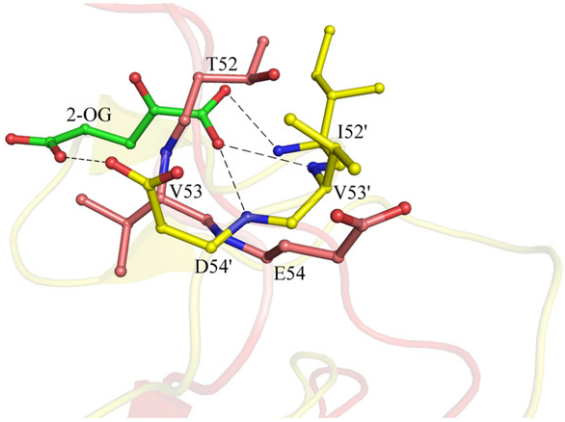

Fig. 5. Comparison of the structure of P_{II} in complex with PipX (red) and the structure of *M. jannaschii* GlnK in complex with 2-OG (yellow; PDB code 2J9E). 2-OG and the residues involved in 2-OG or PipX binding are shown in ball-and-stick format, colored according to atom type. Black broken lines denote polar interactions between 2-OG and GlnK.

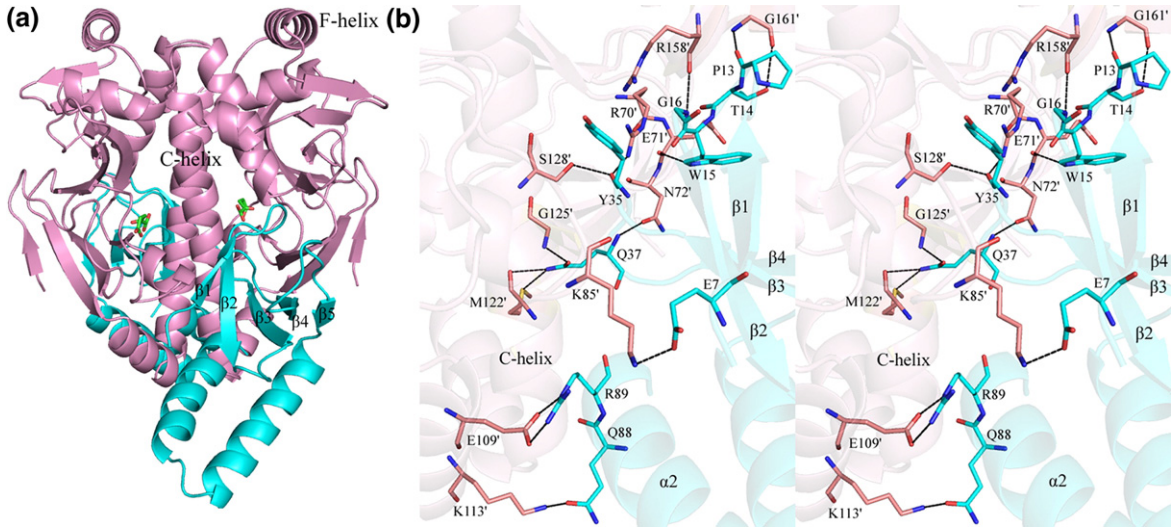

Fig. 6. (a) Simulated three-dimensional model of the NtcA–PipX complex. NtcA (pink) and PipX (cyan) are shown as cartoons. 2-OG molecules are shown as stick models. (b) Stereographic representation of the putative interface between NtcA and PipX. Residues involved in polar interactions are shown in sticks. All broken lines indicate polar interactions.

was somewhat reliable. In the model, each PipX monomer makes extensive interactions with the effector binding domain of one NtcA subunit and with the C-helix and DNA binding domain of the symmetrical subunit (Fig. 6a and b). Multiple alignments revealed that residues Glu7, Tyr9, Thr14, Tyr35, Gln37, Arg38, and Arg57 of PipX at the interface between NtcA and PipX are highly conserved. For the side of NtcA, residues Asn72, Lys85, Glu109, Leu113, Arg124, Ser128, Arg158, and Gly161 are conserved. PipX appears to use a similar site to interact with both P_{II} and NtcA. In the absence of 2-OG, P_{II} might use its 2-OG binding site to interact with PipX and to form a hexameric complex. Upon 2-OG accumulation, this binding site could be occupied by 2-OG, resulting in the dissociation of PipX from P_{II}. The free PipX, most likely as a monomer, would interact with 2-OG-bound NtcA.

This work reveals a novel structure of PipX and dissects the interfaces between P_{II} and PipX. Similarities in the binding site at the T-loop of P_{II} explain why 2-OG causes the release of PipX from P_{II}. In addition, a simulated structure of PipX in complex with 2-OG-bound NtcA indicated that P_{II} and NtcA share a similar binding site on PipX. Taken together, we provide structural insights into the mutually exclusive 2-OG-dependent binding of P_{II} and NtcA by PipX.

Materials and Methods

Protein expression, purification, and crystallization

P_{II} was cloned into the NdeI/XhoI restriction sites of the pET29 expression vector (Novagen). PipX was cloned into the pET28 expression vector with an N-terminal His_6-tag. Plasmids were transformed into *E. coli* strain BL21(DE3) (Novagen) and induced by isopropyl β-D-1-thiogalactopyranoside for overexpression. Cells were harvested after 4 h at 37 °C. Cells containing P_{II} and PipX were mixed and sonicated. After centrifugation, target proteins in the supernatant were purified with a HiTrap nickel-chelating column and a HiLoad 16/60 Superdex 75 column (GE Healthcare) equilibrated with 20 mM Tris–Cl (pH 7.0), 150 mM NaCl, 1 mM $MgCl_2$, 1 mM ethylenediaminetetraacetic acid, and 14 mM β-mercaptoethanol. Protein purity was assessed by SDS-PAGE. A 1-μl protein sample containing 15 mg/ml P_{II}–PipX protein was mixed with a 1-μl reservoir solution of 1.6 M $(NH_4)_2SO_4$ and 0.1 M Tris–Cl (pH 8.5). Crystals were grown in hanging drops equilibrated against the reservoir solution at 16 °C for a week before being flash frozen in liquid nitrogen using reservoir solution with 30% glycerol (vol/vol) as cryoprotectant.

Data collection and processing

X-ray diffraction data were collected at 100 K in a liquid nitrogen stream, using beamline 17U with an MX225 CCD (Marresearch, Germany), at the Shanghai Synchrotron Radiation Facility. The data were integrated and scaled with the program HKL2000.[35]

Structure determination and refinement

Molecular replacement was carried out with MOLREP[36] within the CCP4i[37] suite, using one subunit of the cyanobacterium *Synechococcus* P_{II} (PDB code 1QY7) without the flexible T-loop as model and yielding a solution of one P_{II} molecule in the asymmetric unit. After further improvement of the P_{II} model by rigid-body and restrained refinement using REFMAC5,[38] $F_o - F_c$ density maps were sufficiently clear to trace the backbone of the associated PipX molecule ab initio. After several rounds of

Table 1. Crystal parameters, data collection, and structure refinement

Data collection[a]	
Space group	$P3_21$
Unit cell parameters	
a, *b*, *c* (Å)	70.65, 70.65, 88.54
α, β, χ Unit cell (Å), (°)	90.00, 90.00, 120.00
Resolution range (Å)	50.00–1.90 (1.97–1.90)[a]
Unique reflections	20,553 (1980)
Completeness (%)	99.7 (97.6)
$\langle I/\sigma(I)\rangle$	27.2 (4.2)
R_{merge}[b] (%)	7.3 (35.7)
Average redundancy	8.8 (5.7)
Structure refinement	
Resolution range (Å)	32.81–1.90
R-factor[c]/*R*-free[d] (%)	19.8/24.5
Number of protein atoms	1602
Number of water atoms	133
RMSD[e] bond lengths (Å)	0.015
RMSD bond angles (°)	1.530
Mean *B*-factors (Å^2)	38.52
Ramachandran plot[f] (%)	
Most favored regions (%)	97.42
Additionally allowed regions (%)	2.58
Outliers (%)	0
PDB code	3N5B

[a] The values in parentheses refer to statistics in the highest bin.
[b] $R_{merge} = \sum_{hkl}\sum_i | {}_{II}(hkl) - \langle I(hkl)\rangle | / \sum_{hkl}\sum_{IIi}(hkl)$, where ${}_{II}(hkl)$ is the intensity of an observation, and $\langle I(hkl)\rangle$ is the mean value for its unique reflection. Summations are performed over all reflections.
[c] $R\text{-factor} = \sum_h | F_o(h) - F_c(h) | / \sum_h F_o(h)$, where F_o and F_c are the observed and calculated structure factor amplitudes, respectively.
[d] *R*-free was calculated with 5% of the data excluded from the refinement.
[e] RMSD from ideal values.
[f] Categories were defined by MolProbity.

interactive refinement using REFMAC5 with model building in Coot,[39] we successfully built the PipX model in the final structure. The final model (at 1.90 Å resolution) consisted of one P_{II} chain (A) and one PipX chain (B), showed excellent stereochemistry, and was checked using the programs MolProbity[40] and PROCHECK.[41] Crystallographic parameters are listed in Table 1. All figures were prepared with PyMOL.[42]

Accession numbers

The coordinates and structure factors for the P_{II}–PipX complex have been deposited in the Research Collaboratory for Structural Bioinformatics PDB under accession code 3N5B.

Acknowledgements

We are grateful to the developers of the CCP4 Suite, ESPript, TreeView, and PyMOL, as well as to the Shanghai Synchrotron Radiation Facility. This work was supported by the Ministry of Science and Technology of China (Projects 2006CB910202 and 2006CB806501), the National Natural Science Foundation of China (Program 30870490), and the Agence Nationale de la Recherche (Physico-Chimie du Vivant Program), France.

References

1. Arcondeguy, T., Jack, R. & Merrick, M. (2001). P-II signal transduction proteins, pivotal players in microbial nitrogen control. *Microbiol. Mol. Biol. Rev.* **65**, 80–105.
2. Leigh, J. A. & Dodsworth, J. A. (2007). Nitrogen regulation in bacteria and archaea. *Annu. Rev. Microbiol.* **61**, 349–377.
3. Cheah, E., Carr, P. D., Suffolk, P. M., Vasudevan, S. G., Dixon, N. E. & Ollis, D. L. (1994). Structure of the *Escherichia coli* signal transducing protein P_{II}. *Structure*, **2**, 981–990.
4. Machado Benelli, E., Buck, M., Polikarpov, I., Maltempi de Souza, E., Cruz, L. M. & Pedrosa, F. O. (2002). *Herbaspirillum seropedicae* signal transduction protein P_{II} is structurally similar to the enteric GlnK. *Eur. J. Biochem.* **269**, 3296–3303.
5. Xu, Y., Carr, P. D., Clancy, P., Garcia-Dominguez, M., Forchhammer, K., Florencio, F. *et al.* (2003). The structures of the P_{II} proteins from the cyanobacteria *Synechococcus* sp. PCC 7942 and *Synechocystis* sp. PCC 6803. *Acta Crystallogr. Sect. D*, **59**, 2183–2190.
6. Sakai, H., Wang, H., Takemoto-Hori, C., Kaminishi, T., Yamaguchi, H., Kamewari, Y. *et al.* (2005). Crystal structures of the signal transducing protein GlnK from *Thermus thermophilus* HB8. *J. Struct. Biol.* **149**, 99–110.
7. Nichols, C. E., Sainsbury, S., Berrow, N. S., Alderton, D., Saunders, N. J., Stammers, D. K. & Owens, R. J. (2006). Structure of the P_{II} signal transduction protein of *Neisseria meningitidis* at 1.85 Å resolution. *Acta Crystallogr. Sect. F*, **62**, 494–497.
8. Yildiz, O., Kalthoff, C., Raunser, S. & Kuhlbrandt, W. (2007). Structure of GlnK1 with bound effectors indicates regulatory mechanism for ammonia uptake. *EMBO J.* **26**, 589–599.
9. Mizuno, Y., Berenger, B., Moorhead, G. B. & Ng, K. K. (2007). Crystal structure of *Arabidopsis* P_{II} reveals novel structural elements unique to plants. *Biochemistry*, **46**, 1477–1483.
10. Forchhammer, K. (2008). P-II signal transducers: novel functional and structural insights. *Trends Microbiol.* **16**, 65–72.
11. Forchhammer, K. (2004). Global carbon/nitrogen control by P-II signal transduction in cyanobacteria: from signals to targets. *FEMS Microbiol. Rev.* **28**, 319–333.
12. Ninfa, A. J. & Jiang, P. (2005). P_{II} signal transduction proteins: sensors of alpha-ketoglutarate that regulate nitrogen metabolism. *Curr. Opin. Microbiol.* **8**, 168–173.
13. Jiang, P. & Ninfa, A. J. (2007). *Escherichia coli* P_{II} signal transduction protein controlling nitrogen assimilation acts as a sensor of adenylate energy charge *in vitro*. *Biochemistry*, **46**, 12979–12996.
14. Xu, Y., Cheah, E., Carr, P. D., van Heeswijk, W. C., Westerhoff, H. V., Vasudevan, S. G. & Ollis, D. L. (1998). GlnK, a P_{II}-homologue: structure reveals ATP

binding site and indicates how the T-loops may be involved in molecular recognition. *J. Mol. Biol.* **282**, 149–165.
15. Irmler, A., Sanner, S., Dierks, H. & Forchhammer, K. (1997). Dephosphorylation of the phosphoprotein P (II) in *Synechococcus* PCC 7942: identification of an ATP and 2-oxoglutarate-regulated phosphatase activity. *Mol. Microbiol.* **26**, 81–90.
16. Zhang, Y., Pu, H., Wang, Q. S., Cheng, S., Zhao, W. X., Zhang, Y. & Zhao, J. D. (2007). P_{II} is important in regulation of nitrogen metabolism but not required for heterocyst formation in the cyanobacterium *Anabaena* sp. PCC 7120. *J. Biol. Chem.* **282**, 33641–33648.
17. Atkinson, M. R. & Ninfa, A. J. (1999). Characterization of the GlnK protein of *Escherichia coli*. *Mol. Microbiol.* **32**, 301–313.
18. Zhang, Y. & Zhao, J. (2008). P_{II}, the key regulator of nitrogen metabolism in the cyanobacteria. *Sci. China Ser. C: Life Sciences*, **51**, 1056–1065.
19. Stanier, R. Y. & Cohen-Bazire, G. (1977). Phototrophic prokaryotes: the cyanobacteria. *Annu. Rev. Microbiol.* **31**, 225–274.
20. Burillo, S., Luque, I., Fuentes, I. & Contreras, A. (2004). Interactions between the nitrogen signal transduction protein P_{II} and *N*-acetyl glutamate kinase in organisms that perform oxygenic photosynthesis. *J. Bacteriol.* **186**, 3346–3354.
21. Espinosa, J., Forchhammer, K., Burillo, S. & Contreras, A. (2006). Interaction network in cyanobacterial nitrogen regulation: PipX, a protein that interacts in a 2-oxoglutarate dependent manner with P_{II} and NtcA. *Mol. Microbiol.* **61**, 457–469.
22. Osanai, T., Sato, S., Tabata, S. & Tanaka, K. (2005). Identification of PamA as a P_{II}-binding membrane protein important in nitrogen-related and sugar-catabolic gene expression in *Synechocystis* sp. PCC 6803. *J. Biol. Chem.* **280**, 34684–34690.
23. Llacer, J. L., Contreras, A., Forchhammer, K., Marco-Marin, C., Gil-Ortiz, F., Maldonado, R. *et al.* (2007). The crystal structure of the complex of P-II and acetylglutamate kinase reveals how P-II controls the storage of nitrogen as arginine. *Proc. Natl Acad. Sci. USA*, **104**, 17644–17649.
24. Espinosa, J., Forchhammer, K. & Contreras, A. (2007). Role of the *Synechococcus* PCC 7942 nitrogen regulator protein PipX in NtcA-controlled processes. *Microbiology*, **153**, 711–718.
25. Mizuno, Y., Moorhead, G. B. & Ng, K. K. (2007). Structural basis for the regulation of *N*-acetylglutamate kinase by P_{II} in *Arabidopsis thaliana*. *J. Biol. Chem.* **282**, 35733–35740.
26. Conroy, M. J., Durand, A., Lupo, D., Li, X. D., Bullough, P. A., Winkler, F. K. & Merrick, M. (2007). The crystal structure of the *Escherichia coli* AmtB–GlnK complex reveals how GlnK regulates the ammonia channel. *Proc. Natl Acad. Sci. USA*, **104**, 1213–1218.
27. Gruswitz, F., O(Connell, J., III & Stroud, R. M. (2007). Inhibitory complex of the transmembrane ammonia channel, AmtB, and the cytosolic regulatory protein, GlnK, at 1.96 Å. *Proc. Natl Acad. Sci. USA*, **104**, 42–47.
28. Holm, L. & Sander, S. (1998). Touring protein fold space with Dali/FSSP. *Nucleic Acids Res.* **26**, 316–319.
29. Palinska, K. A., Laloui, W., Bedu, S., Loiseaux-de Goer, S., Castets, A. M., Rippka, R. & de Marsac, N. T. (2002). The signal transducer P-II and bicarbonate acquisition in *Prochlorococcus marinus* PCC 9511, a marine cyanobacterium naturally deficient in nitrate and nitrite assimilation. *Microbiology*, **148**, 2405–2412.
30. Schwarzenbacher, R., von Delft, F., Abdubek, P., Ambing, E., Biorac, T., Brinen, L. S. *et al.* (2004). Crystal structure of a putative P_{II}-like signaling protein (TM0021) from *Thermotoga maritima* at 2.5 angstrom resolution. *Proteins Struct. Funct. Bioinf.* **54**, *810–813.*
31. Forchhammer, K. & Hedler, A. (1997). Phosphoprotein P_{II} from cyanobacteria—analysis of functional conservation with the P_{II} signal-transduction protein from *Escherichia coli*. *Eur. J. Biochem.* **244**, 869–875.
32. Zhao, M. X., Jiang, Y. L., He, Y. X., Chen, Y. F., Teng, Y. B., Chen, Y. *et al.* (2010). Structural basis for the allosteric control of the global transcription factor NtcA by the nitrogen starvation signal 2-oxoglutarate. *Proc. Natl Acad. Sci. USA* **107**, *12487–12492.*
33. Dominguez, C., Boelens, R. & Bonvin, A. M. (2003). HADDOCK: a protein–protein docking approach based on biochemical or biophysical information. *J. Am. Chem. Soc.* **125**, 1731–1737.
34. de Vries, S. J., van Dijk, A. D. & Bonvin, A. M. (2006). WHISCY: what information does surface conservation yield? Application to data-driven docking. *Proteins*, **63**, 479–489.
35. Otwinowski, Z. & Minor, W. (1997). Processing of X-ray diffraction data collected in oscillation mode. *Macromol. Crystallogr.* **276**, 307–326.
36. Vagin, A. & Teplyakov, A. (1997). MOLREP: an automated program for molecular replacement. *J. Appl. Crystallogr.* **30**, 1022–1025.
37. Collaborative Computational Project, No. 4 (1994). The CCP4 suite: programs for protein crystallography. *Acta Crystallogr. Sect. D*, **50**, 760–763.
38. Murshudov, G. N., Vagin, A. A. & Dodson, E. J. (1997). Refinement of macromolecular structures by the maximum-likelihood method. *Acta Crystallogr. Sect. D*, **53**, 240–255.
39. Emsley, P. & Cowtan, K. (2004). Coot: model-building tools for molecular graphics. *Acta Crystallogr. Sect. D*, **60**, 2126–2132.
40. Davis, I., Leaver-Fay, A., Chen, V., Block, J., Kapral, G., Wang, X. *et al.* (2007). MolProbity: all-atom contacts and structure validation for proteins and nucleic acids. *Nucleic Acids Res.* **35**, W375–W383.
41. Laskowski, R., Macarthur, M., Moss, D. & Thornton, J. (1993). PROCHECK—a program to check the stereochemical quality of protein structures. *J. Appl. Crystallogr.* **26**, 283–291.
42. DeLano, W. (2002). *The PyMOL Molecular Graphics System.*De Lano Scientific, San Carlos, CA. http://www.pymol.org.